Existence of a magnetization plateau in a class of exactly solvable Ising–Heisenberg chains

2003 J. Phys.: Condens. Matter 15 4519

(http://iopscience.iop.org/0953-8984/15/26/302)

INSTITUTE OF PHYSICS PUBLISHING JOURNAL OF PHYSICS: CONDENSED MATTER

J. Phys.: Condens. Matter **15** (2003) 4519–4534 PII: S0953-8984(03)59252-9

Existence of a magnetization plateau in a class of exactly solvable Ising–Heisenberg chains

Jozef Strečka and Michal Jaščur

Faculty of Science, Department of Theoretical Physics and Astrophysics, P J Šafárik University, Moyzesova 16, 041 54 Košice, Slovak Republic

E-mail: jozkos@pobox.sk and jascur@kosice.upjs.sk

Received 5 February 2003, in final form 22 May 2003
Published 20 June 2003
Online at stacks.iop.org/JPhysCM/15/4519

Abstract

The mapping transformation technique is applied to obtain exact results for the spin-1/2 and spin-S ($S = 1/2, 1$) Ising–Heisenberg antiferromagnetic chain in the presence of an external magnetic field. Within this scheme, a field-induced first-order metamagnetic phase transition resulting in multiplateau magnetization curves is investigated in detail. It is found that the scenario of the plateau formation depends fundamentally on the ratio between Ising and Heisenberg interaction parameters, as well as on the strength of the XXZ Heisenberg exchange anisotropy.

1. Introduction

Quantum antiferromagnetism in lower dimensions is one of the most fascinating subjects in condensed matter physics. In particular, the antiferromagnetic quantum Heisenberg chains (AFQHC) with small spins have attracted much attention on account of the rich quantum behaviour they display. Nevertheless, due to strong quantum fluctuations the classical Néel state is no longer an eigenstate of the Hamiltonian, and thus more interesting quantum phases should be expected to occur in the ground state. The nature of these phases, however, basically depends on the spin value of atoms. In fact, as conjectured by Haldane [1] in 1983, the integer spin AFQHC have a finite energy gap between the ground state and the first excited state, while the half-odd integer ones possess a gapless excitation spectrum.

Another striking feature of the AFQHC is the appearance of fractional magnetization plateaus in the magnetization process. Extending the original Lieb–Schultz–Mattis theorem [2] Oshikawa, Yamanaka and Affleck (OYA) [3] argued that the magnetization per site m can be topologically quantized as $p(S_u - m) =$ integer, where p is a period of ground state in the thermodynamic limit and S_u denotes the total spin of an elementary unit. However, this condition represents just the necessary condition for plateau-state formation and does not directly prove its existence. It is therefore of interest to investigate how the plateau state is related to the periodicity of a specific model [4]. Moreover, from the theoretical viewpoint

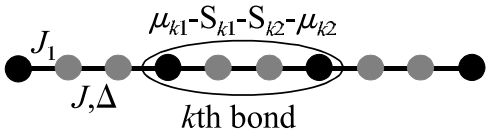

Figure 1. Part of the doubly decorated mixed-spin chain. The black circles denote the spin-1/2 Ising atoms of sublattice A and the grey ones represent the decorating spin-S Heisenberg atoms of sublattice B. The ellipse demarcates a typical bond described by the Hamiltonian $\hat{\mathcal{H}}_k$ introduced in equation (2).

the plateau state can also be regarded as a spin-gap state. Hence, the zero-temperature magnetization curves with plateaus bring an insight into the ground-state properties of the system, since the field-induced spin gaps reflect the gapped excitation spectrum.

Despite an extensive theoretical effort focused on AFQHC, there still exist only a few exactly solvable models with pure Heisenberg exchange interactions [5], especially for mixed-spin chains [6]. On the other hand, an exact solution for chains with alternating Ising- and Heisenberg-type exchange interactions can be attained in a less sophisticated manner. Indeed, the exact solution for the Ising–Heisenberg bond alternating chain (originally proposed and solved by Lieb *et al* [2]), has recently been successfully generalized to the case of anisotropic Heisenberg interaction [7]. In order to avoid mathematical complexities connected with the noncommutability of relevant spin operators, we will introduce in this paper another class of Ising–Heisenberg chains (with period $p = 3$) that can be treated exactly within the mapping transformation method. However, the considered model naturally enables us to analyse in detail the mutual competition between Ising- and Heisenberg-type interactions and, moreover, it also proves to be very useful in view of the confirmation of multiplateau magnetization curves by an exact calculation.

This paper is organized as follows. In section 2 a detailed description of the model as well as the fundamental aspects of transformation technique are presented. In section 3 we are concerned with the analysis of the most interesting numerical results for typical spin cases and finally, in section 4, some concluding remarks are given.

2. Model and method

In this paper we will study a mixed spin-1/2 and spin-S ($S = 1/2, 1$) Ising–Heisenberg chain in the presence of an external magnetic field. The structure of the considered mixed-spin chain is depicted in figure 1, where the black circles denote the spin-1/2 atoms and the grey ones represent the spin-S atoms. The total Hamiltonian of the system is given by:

$$\hat{\mathcal{H}} = J \sum_{i,j} [\Delta(\hat{S}_i^x \hat{S}_j^x + \hat{S}_i^y \hat{S}_j^y) + \hat{S}_i^z \hat{S}_j^z] + J_1 \sum_{k,l} \hat{S}_k^z \hat{\mu}_l^z - H_A \sum_l \hat{\mu}_l^z - H_B \sum_k \hat{S}_k^z, \tag{1}$$

where $\hat{\mu}_l^z$ and $\hat{S}_k^\alpha$ ($\alpha = x, y, z$) denote the well-known components of standard spin-1/2 and spin-S ($S = 1/2, 1$) operators respectively. The parameter J stands for the Heisenberg interaction between nearest-neighbour spin-S atoms (the grey atoms) and Δ is the anisotropy parameter that allows control of the anisotropic XXZ interaction between an easy-axis regime ($\Delta < 1$) and an easy-plane regime ($\Delta > 1$). Furthermore, the interaction parameter J_1 describes the Ising-type exchange interaction between pairs of nearest-neighbour spin-1/2 and spin-S atoms, and finally the terms incorporating H_A and H_B respectively describe the coupling of spin-1/2 atoms and spin-S atoms to an external magnetic field. As we can see from figure 1, all pairs of nearest-neighbour Heisenberg atoms are surrounded by Ising-type

atoms only, thus the model under investigation can also be viewed as an Ising model the bonds of which are doubly decorated by the Heisenberg atoms. In view of further manipulations, it is useful to rewrite the total Hamiltonian $\hat{\mathcal{H}}$ as a sum of the bond Hamiltonians, i.e. $\hat{\mathcal{H}} = \sum_{k=1}^{N} \hat{\mathcal{H}}_k$, where N denotes the total number of Ising-type atoms and the summation runs over all bonds of the original (undecorated) chain. The bond Hamiltonian $\hat{\mathcal{H}}_k$ contains all the interaction terms associated with the kth couple of Heisenberg atoms (see figure 1), and it is given by

$$\hat{\mathcal{H}}_k = J[\Delta(\hat{S}^x_{k1}\hat{S}^x_{k2} + \hat{S}^y_{k1}\hat{S}^y_{k2}) + \hat{S}^z_{k1}\hat{S}^z_{k2}] + J_1(\hat{S}^z_{k1}\hat{\mu}^z_{k1} + \hat{S}^z_{k2}\hat{\mu}^z_{k2}) - H_B(\hat{S}^z_{k1} + \hat{S}^z_{k2}) - H_A(\hat{\mu}^z_{k1} + \hat{\mu}^z_{k2})/2. \tag{2}$$

Now, exploiting the usual commutation relation for the bond Hamiltonians (i.e. $[\hat{\mathcal{H}}_k, \hat{\mathcal{H}}_j] = 0$, for $k \neq j$), the partition function of the system can be partially factorized, namely

$$\mathcal{Z} = \mathrm{Tr}_{\{\mu\}} \prod_{k=1}^{N} \mathrm{Tr}_{S_{k1}} \mathrm{Tr}_{S_{k2}} \exp(-\beta\hat{\mathcal{H}}_k). \tag{3}$$

In the above, $\beta = (k_B T)^{-1}$, k_B being Boltzmann constant and T the absolute temperature. $\mathrm{Tr}_{\{\mu\}}$ means a trace over the degrees of freedom of the Ising spins and $\mathrm{Tr}_{S_{k1}}\mathrm{Tr}_{S_{k2}}$ denotes a trace over the kth couple of Heisenberg spins. At this stage one can easily observe that the structure of relation (3) implies the possibility of introducing the decoration–iteration mapping transformation [8]

$$\mathrm{Tr}_{S_{k1}} \mathrm{Tr}_{S_{k2}} \exp(-\beta\hat{\mathcal{H}}_k) = A \exp[\beta R \mu^z_{k1}\mu^z_{k2} + \beta H_0(\mu^z_{k1} + \mu^z_{k2})/2]. \tag{4}$$

As usual, the unknown transformation parameters A, R and H_0 can be attained by taking into account the remaining degrees of freedom of both Ising spins (μ_{k1} and μ_{k2}). In this way one obtains the following expressions for the transformation parameters A, R and H_0:

$$A = (V_1 V_2 V_3^2)^{1/4}, \qquad \beta R = \ln\left(\frac{V_1 V_2}{V_3^2}\right), \qquad \beta H_0 = \beta H_A - \ln\left(\frac{V_1}{V_2}\right), \tag{5}$$

where the functions V_1, V_2 and V_3 depend on the spin value of Heisenberg atoms, as well as on the parameters of the Hamiltonian (1), and they are summarized for both investigated spin cases in the appendix.

Here, one should emphasize that the mapping relations (4), (5) enable us to transform the Ising–Heisenberg mixed-spin chain onto a simple spin-1/2 Ising chain with an effective exchange parameter R, placed in an external magnetic field of magnitude H_0. Indeed, substituting (4) into (3) gives the following equality

$$\mathcal{Z}(\beta, J, J_1, \Delta, H_A, H_B) = A^N \mathcal{Z}_0(\beta, R, H_0), \tag{6}$$

which relates the partition function of the Ising–Heisenberg chain $\mathcal{Z}$ and that of the spin-1/2 Ising chain $\mathcal{Z}_0$. Since the explicit expression for $\mathcal{Z}_0$ is well known [9], we can then straightforwardly calculate all relevant thermodynamic quantities. For example, the Gibbs free energy $\mathcal{G}$ of the mixed-spin Ising–Heisenberg chain is given by

$$\mathcal{G} = \mathcal{G}_0 - N k_B T \ln A, \tag{7}$$

where $\mathcal{G}_0 = -k_B T \ln \mathcal{Z}_0$ denotes the Gibbs free energy of the corresponding spin-1/2 Ising chain. Next, by differentiating the Gibbs free energy $\mathcal{G}$ with respect to H_A and H_B respectively, one directly obtains the solution for the total sublattice magnetization. Of course, other thermodynamic quantities can also be calculated on the basis of familiar thermodynamic relations, e.g. the entropy S and the specific heat C can be calculated from

$$S = -\left(\frac{\partial G}{\partial T}\right)_H, \qquad C = -T\left(\frac{\partial^2 G}{\partial T^2}\right)_H. \tag{8}$$

Nevertheless, a similar thermodynamic approach cannot be used for the calculation of other important quantities such as staggered magnetization, quadrupolar momentum or some correlations. Fortunately, equation (6) in conjunction with the transformation formula (4) allows, after some elementary algebra, the derivation of following exact spin identities [10]

$$\begin{aligned}&\langle f_1(\hat{\mu}_i^z, \hat{\mu}_j^z, \ldots, \hat{\mu}_k^z,)\rangle = \langle f_1(\hat{\mu}_i^z, \hat{\mu}_j^z, \ldots, \hat{\mu}_k^z,)\rangle_0,\\ &\langle f_2(\hat{S}_{k1}^{\alpha}, \hat{S}_{k2}^{\gamma}, \hat{\mu}_{k1}^z, \hat{\mu}_{k2}^z)\rangle = \left\langle \frac{\mathrm{Tr}_{S_{k1}}\mathrm{Tr}_{S_{k2}} f_2(\hat{S}_{k1}^{\alpha}, \hat{S}_{k2}^{\gamma}, \hat{\mu}_{k1}^z, \hat{\mu}_{k2}^z)\exp(-\beta\hat{\mathcal{H}}_k)}{\mathrm{Tr}_{S_{k1}}\mathrm{Tr}_{S_{k2}}\exp(-\beta\hat{\mathcal{H}}_k)}\right\rangle,\end{aligned} \tag{9}$$

with arbitrary function f_1 depending exclusively on Ising spin variables and the function f_2 depending on the spin variables from the kth bond only. The superscripts $\alpha, \gamma \equiv (x, y, z)$ label the spatial components of spin operators, and finally the symbols $\langle\cdots\rangle$ and $\langle\cdots\rangle_0$ stand for the standard ensemble average in the Ising–Heisenberg and its equivalent simple Ising model respectively. However, the above spin identities considerably simplify the calculation of a large number of quantities. Indeed, for the reduced sublattice magnetization (m_A^z, m_B^z), the total single-site magnetization m and the staggered sublattice magnetization (m_A^s, m_B^s), one attains, after straightforward algebra,

$$\begin{aligned}&m_A^z \equiv \tfrac{1}{2}\langle\hat{\mu}_{k1}^z + \hat{\mu}_{k2}^z\rangle = \tfrac{1}{2}\langle\hat{\mu}_{k1}^z + \hat{\mu}_{k2}^z\rangle_0 \equiv m_0,\\ &m_B^z \equiv \tfrac{1}{2}\langle\hat{S}_{k1}^z + \hat{S}_{k2}^z\rangle = (V_4/V_1 - V_5/V_2 + 2V_6/V_3)/2\\ &\qquad\qquad - 2m_0(V_4/V_1 + V_5/V_2) + 2\varepsilon_0(V_4/V_1 - V_5/V_2 - 2V_6/V_3),\\ &m \equiv (m_A^z + 2m_B^z)/3,\\ &m_A^s \equiv \tfrac{1}{2}\langle\hat{\mu}_{k1}^z - \hat{\mu}_{k2}^z\rangle = \tfrac{1}{2}\langle\hat{\mu}_{k1}^z - \hat{\mu}_{k2}^z\rangle_0 \equiv m_0^s,\\ &m_B^s \equiv \tfrac{1}{2}\langle\hat{S}_{k1}^z - \hat{S}_{k2}^z\rangle = -m_0^s V_7/V_3.\end{aligned} \tag{10}$$

In the above, m_0, m_0^s and ε_0 represent the reduced magnetization, staggered magnetization and nearest-neighbour correlation of the corresponding undecorated Ising chain and the coefficients V_1–V_7 are listed for both investigated spin cases in the appendix.

Finally, let us define some pair correlation functions and the quadrupolar momentum, which are also very useful for understanding of magnetic properties of the system, namely

$$\begin{aligned}&q_{hh}^{xx} \equiv \langle\hat{S}_{k1}^x\hat{S}_{k2}^x\rangle \equiv \langle\hat{S}_{k1}^y\hat{S}_{k2}^y\rangle, \qquad q_{hh}^{zz} \equiv \langle\hat{S}_{k1}^z\hat{S}_{k2}^z\rangle, \qquad q_{ii}^{zz} \equiv \langle\hat{\mu}_{k1}^z\hat{\mu}_{k2}^z\rangle \equiv \varepsilon_0,\\ &q_{ih}^{zz} \equiv \tfrac{1}{2}\langle\hat{S}_{k1}^z\hat{\mu}_{k1}^z + \hat{S}_{k2}^z\hat{\mu}_{k2}^z\rangle, \qquad \eta \equiv \tfrac{1}{2}\langle(\hat{S}_{k1}^z)^2 + (\hat{S}_{k2}^z)^2\rangle.\end{aligned} \tag{11}$$

In these equations, the subscripts denote the type of atom and superscripts the space direction. One should also notice that the definition of the parameter η is obviously meaningful for $S \geqslant 1$ only. Although, the derivation of relevant equations for these quantities is straightforward, the calculation procedure by itself is rather lengthy and tedious, thus the details are not presented here.

3. Numerical results and discussion

Before discussing the most interesting numerical results, it is worth mentioning that some preliminary results for the ferromagnetic version of the model ($J < 0$, $J_1 < 0$) have already been published by the present authors elsewhere [11]. For this reason, in this paper we will restrict our attention to the doubly decorated Ising–Heisenberg chain with antiferromagnetic (AF) interactions only (i.e. $J > 0$, $J_1 > 0$). The particular attention is focused on the ground-state analysis and the appearance of plateaus in the chains with different decorating spin S. Among other matters, we will directly prove the existence of a double-plateau magnetization curve in the spin $S = 1/2$ chain; more precisely, the magnetization curve with plateaus at $m = 0$ and $1/6$. On the other hand, in the spin $S = 1$ chain a greater diversity of magnetization

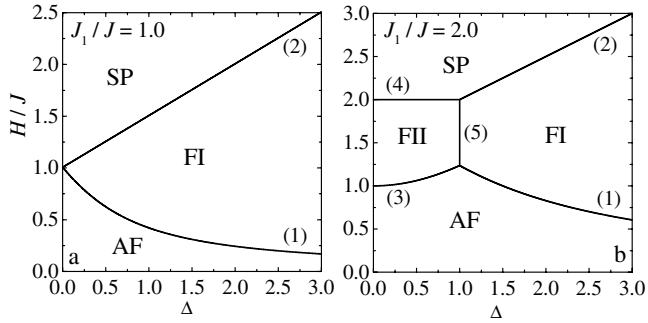

Figure 2. Ground-state phase boundaries in the Δ–H/J plane for $J_1/J = 1.0$ and 2.0.

processes will be confirmed; in fact, we will prove the existence of double-plateau ($m = 0$ and $1/2$), triple-plateau ($m = 0$, $1/6$ and $1/2$) and quadruple-plateau ($m = 0$, $1/6$, $1/3$ and $1/2$) magnetization curves.

In addition, since each couple of Heisenberg atoms is surrounded by the Ising atoms only, the relevant spin deviations cannot propagate through the Ising bonds and therefore, the quantum fluctuations are necessarily localized within the unit cell (within the four-spin cluster consisting of the Heisenberg spin pair and its nearest-neighbour Ising spins). Owing to this fact, the observed plateaus cannot be considered as OYA plateaus, i.e. plateaus with a collective eigenstate extending over the whole chain. Nevertheless, it is interesting to note that all observed fractional magnetizations satisfy the OYA condition for $p = 6$ (the period of translational symmetry should be twice as large as the periodicity of Hamiltonian as a consequence of an AF nature of the ground state).

3.1. Spin $S = 1/2$ chain

We begin our analysis by considering the effect of exchange anisotropy Δ and uniform magnetic field (i.e. $H_A = H_B = H$) on the ground-state phase boundaries of the spin $S = 1/2$ chain. For this purpose, we have displayed in figure 2 some typical ground-state phase diagrams in the Δ–H/J plane for $J_1/J = 1.0$ and 2.0. As one can see from this figure, the relevant phase boundaries separate three or four distinct phases, namely the AF, ferrimagnetic I (FI), ferrimagnetic II (FII) and saturated paramagnetic (SP) phases. One also observes that both ferrimagnetic phases (FI and FII) represent an intermediate phase between the AF and SP phases occurring due to the first-order metamagnetic transition. As we have already mentioned, different phases can be distinguished by analysing the magnetization and the correlation functions at $T = 0$. In this way one finds the following ground-state results for particular phases.

The AF phase:

$$(q_{hh}^{xx}, q_{hh}^{zz}, q_{ih}^{zz}, q_{ii}^{zz}, m_A^s, m_B^s) = (-J\Delta Q^{-1}, -1/4, -J_1 Q^{-1}, -1/4, 1/2, -2J_1 Q^{-1});$$

where we have defined the function $Q = 4\sqrt{J_1^2 + (J\Delta)^2}$, in order to write the relevant expressions in more abbreviated and elegant form.

Ferrimagnetic phase I (FI):

$$(q_{hh}^{xx}, q_{hh}^{zz}, q_{ih}^{zz}, q_{ii}^{zz}, m_A^z, m_B^z, m) = (-1/4, -1/4, 0, 1/4, 1/2, 0, 1/6).$$

Ferrimagnetic phase II (FII):

$$(q_{hh}^{xx}, q_{hh}^{zz}, q_{ih}^{zz}, q_{ii}^{zz}, m_A^z, m_B^z, m) = (0, 1/4, -1/4, 1/4, -1/2, 1/2, 1/6).$$

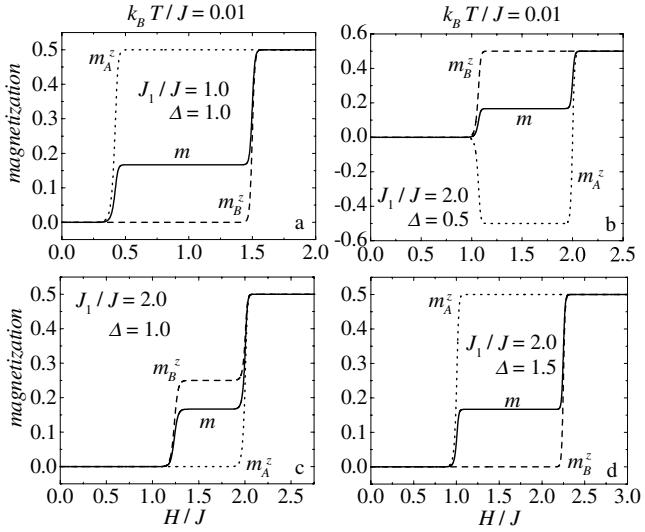

Figure 3. Low-temperature ($k_B T/J = 0.01$) magnetization curves for: (a) $J_1/J = 1.0$ and $\Delta = 1.0$; (b)–(d) $J_1/J = 2.0$ and $\Delta = 0.5$, 1.0, 1.5. The solid and dotted (dashed) curves represent the total magnetization per one site and the single-site magnetization of the Ising (Heisenberg) sublattice respectively.

The SP paramagnetic phase:

$$(q_{hh}^{xx}, q_{hh}^{zz}, q_{ih}^{zz}, q_{ii}^{zz}, m_A^z, m_B^z, m) = (0, 1/4, 1/4, 1/4, 1/2, 1/2, 1/2).$$

Moreover, it is also noteworthy that all ground-state phase boundaries can be expressed analytically as follows (see figure 2):

(a) for $J_1/J \leqslant 1.0$

$$\text{(1) } H/J = \sqrt{\Delta^2 + (J_1/J)^2} - \Delta, \qquad \text{(2) } H/J = (\Delta + J_1/J)/2 + 1/2, \tag{12}$$

(b) $J_1/J > 1.0$

$$\begin{aligned} &\text{(1) } H/J = \sqrt{\Delta^2 + (J_1/J)^2} - \Delta, \qquad \text{(2) } H/J = (\Delta + J_1/J)/2 + 1/2, \\ &\text{(3) } H/J = \sqrt{\Delta^2 + (J_1/J)^2} - J_1/J + 1, \qquad \text{(4) } H/J = J_1/J, \\ &\text{(5) } \Delta = J_1/J - 1. \end{aligned} \tag{13}$$

In order to demonstrate the diversity of the magnetization process, we have plotted in figure 3 the low-temperature magnetization curves for various exchange anisotropies Δ. Detailed examination of these dependences reveals that the mechanism of the magnetization process depends basically on the ratio between Ising and Heisenberg interaction constants, and more specifically on whether $J_1/J \leqslant 1.0$ or $J_1/J > 1.0$. In the former case, the plateau state arises due to the alignment of the Ising spins towards the direction of the external field (FI phase) regardless of the anisotropy strength Δ (see figure 3(a)). Naturally, in this case there is no other possibility for the formation of an intermediate plateau. On the other hand, in the case of $J_1/J > 1.0$ the metamagnetic transition to the FI phase can be observed for the stronger anisotropies Δ only (see figure 3(d)), while for the weaker anisotropies the FII phase becomes the stable one. In this phase, the Heisenberg (Ising) spins align parallel (antiparallel) with respect to the direction of the external field as is apparent from figure 3(b). Moreover, the situation for the most interesting point at which both intermediate phases (FI and FII) coexist

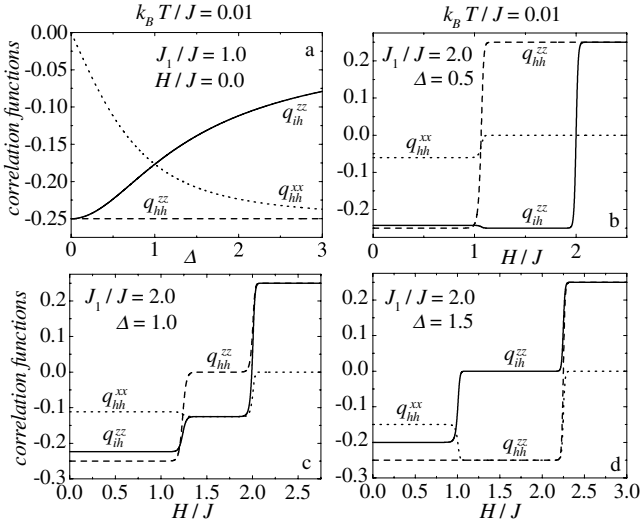

Figure 4. Low-temperature behaviour ($k_B T/J = 0.01$) of several correlation functions: q_{hh}^{zz} and q_{ii}^{zz} (dashed curves), q_{hh}^{xx} (dotted curves) and q_{ih}^{zz} (solid curves). (a) Plot of the correlation functions against the anisotropy Δ for the system without an external field; (b)–(d) field dependence of the correlation functions depicted for $J_1/J = 2.0$ and various anisotropies $\Delta = 0.5$, 1.0 and 1.5.

is depicted in figure 3(c). Referring to this plot, the coexistence of both ferrimagnetic phases is also reflected in the mixed feature of the magnetization curve (compare magnetization curve from figure 3(c) with those in figures 3(b) and (d)).

In order to enable an independent check of the magnetization scenario, we have also studied the relevant low-temperature dependences of the nearest-neighbour correlation functions introduced in equation (11). In figure 4(a), the variations of the correlation functions with anisotropy Δ are shown for the system without an external magnetic field. As one can see, the correlation function q_{hh}^{zz} between Heisenberg spins takes its saturation value irrespective of Δ, which means that all nearest-neighbour Heisenberg spin pairs align antiparallel with respect to each other. Moreover, the saturated value of correlation $q_{ii}^{zz} = -1/4$ indicates a perfect AF alignment also in the Ising sublattice (between third nearest-neighbour Ising spins). Contrary to this behaviour, the perfect antiparallel alignment between Ising and Heisenberg spins is destroyed as Δ increases from zero (see the correlation q_{ih}^{zz}). Hence, the Ising and Heisenberg spins are oriented randomly with respect to each other, the degree of randomness being greater the stronger the exchange anisotropy Δ. In addition, it is clear that the anisotropy term Δ is also responsible for the onset of an interesting short-range ordering (nonzero q_{hh}^{xx}) in the xy plane. Anyway, the value of correlation q_{hh}^{xx} can be thought of as a measure of the strength of local quantum fluctuations appearing in the spin system. Furthermore, in figures 4(b)–(d) we have displayed the field dependences of the correlation functions corresponding to the magnetization curves from figures 3(b)–(d). The depicted behaviour for the correlation functions is in complete agreement with results for the magnetization curves, and, moreover, it enables better understanding of the magnetic ordering in the relevant phases. As a typical example we can mention the ferrimagnetic phases. Although the total magnetization of both the FI and FII phases is the same, the results for other quantities indicate a fundamental difference between them. In fact, in the FI phase the pairs of Heisenberg spins create singlet dimers and thus they do not contribute to the total magnetization which is nonzero due to the

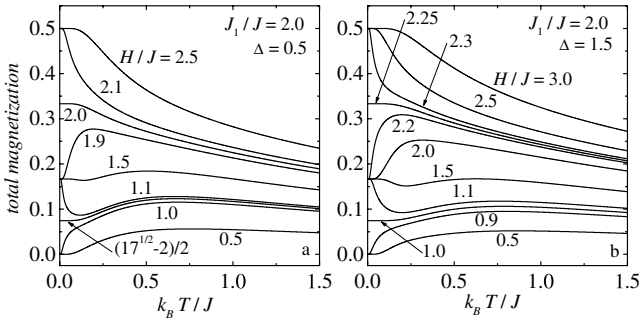

Figure 5. Thermal variations of the total magnetization for some typical values of the external field, $J_1/J = 2.0$ and two selected anisotropies $\Delta = 0.5$ and 1.5, respectively.

fully polarized Ising spins only, as already stated. This observation would suggest that the formation of an FI plateau state should be based on the quantum mechanism with a significant influence of local quantum fluctuations. In contrast to this, the FII phase represents the standard ferrimagnetically ordered phase usually observed in pure Ising systems. Indeed, the generation of the FII plateau state is nothing but the gapped excitation from the Néel state, implying a magnetization process with a 'classical' Ising-like mechanism. Finally, one should notice that after exceeding the saturation field given by conditions (12) and (13), the ground state becomes fully polarized (SP phase) and all spins are aligned in the direction of the external field.

Now, let us investigate the finite-temperature behaviour of the system. Firstly, we take a closer look at the thermal dependences of total magnetization that are shown in figure 5. As we can see, the initial value of total magnetization takes one of three possible values $m = 0$, $1/6$ or $1/2$ for the AF, FI (FII) or SP phase respectively. Furthermore, there are two special cases which correspond to the coexistence of the relevant phases. In these cases, we have obviously obtained $m = 1/12$ or $1/3$ at $T = 0$. It is also easy to observe here that the most interesting dependences appear for external fields from the neighbourhood of phase boundaries. Hence, the observed rapid increase (decrease) of the magnetization can be attributed to the thermal excitations of huge number of spins which occur due to the competitive influence of both phases.

For completeness, we have also plotted the entropy (figure 6(a)) and the specific heat (figures 6(b)–(d)) as a function of temperature. As one can expect, the entropy of the system does not vanish for the boundary external-field values $H/J = 1.0$ and 2.25, at which the relevant phases coexist in the ground state (see figure 6(a)). However, we should mention that for any other external fields the entropy vanishes as the temperature goes to zero. Another quantity which is also interesting from the experimental point of view is the specific heat. The thermal variations of this quantity are depicted in figure 6(b) for the same values of H/J as for entropy in figure 6(a). The displayed behaviour indicates a round Schottky-type maximum, whereas the stronger the external field, the flatter and broader the maximum. Apart from this trivial finding, one can also observe the double-peak specific heat curves (see figures 6(c) and (d)). The first peak which occurs in the specific heat curve at lower temperature is evidently closely related to the rapid variation of the magnetization (compare figures 6(c), (d) with 5(b)). Moreover, it turns out that the maximum of this peak can be located approximately in the middle of the ferrimagnetic region (in our case around $H/J \approx 1.5$). On the other hand, the second peak may be thought as a Schottky-like peak resulting from the AF short-range order. Indeed, the relevant thermal dependences for the nearest-neighbour correlations strongly support this statement.

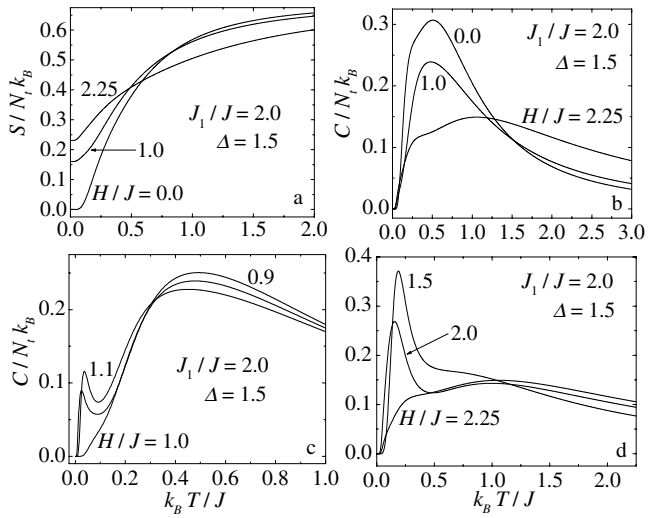

Figure 6. Thermal behaviour of the system for $J_1/J = 2.0$, $\Delta = 1.5$ and several values of external field: (a) entropy plot versus temperature; (b)–(d) variations of the specific heat with temperature.

In the following subsection we examine the spin $S = 1$ chain in order to clarify the influence of decorating spin on the magnetic properties of the system.

3.2. Spin $S = 1$ chain

We start our discussion once again with an analysis of the ground state. In order to establish correct ground-state phase boundaries all relevant quantities have been examined in detail. From this analysis one can conclude that depending on the ratio between J_1, $J(\Delta)$ and H, a total of six different phases can appear in the ground state (see ground-state phase diagrams in figures 7(a) and 9(a), (b)). In this subsection, we will first describe details of the spin ordering emerging in the appropriate ground-state phases, and then we will show how the scenario of the magnetization process depends on the parameters of the model.

In the AF phase one finds a perfect AF alignment in the Ising sublattice (i.e. $m_A^s = 1/2$ and $q_{ii}^{zz} = -1/4$) regardless of the strength of the exchange anisotropy Δ. Accordingly, the relevant spin order in the Ising sublattice is completely identical to that in the AF phase of the spin $S = 1/2$ chain. Nevertheless, in contrast to the spin $S = 1/2$ case, the antiparallel alignment between nearest-neighbour Heisenberg spins is weakened along the z-axis as Δ increases from zero. In fact, the correlation q_{hh}^{zz} tends monotonically from its classical Ising value $q_{hh}^{zz} = -1$ at $\Delta = 0$ to $q_{hh}^{zz} = -1/2$ for large Δ (see e.g. figure 8(a)). In addition, one can also easily prove the validity of relation $\eta = |q_{hh}^{zz}|$ in the whole AF region. This observation would suggest that Δ supports the spin reorientation of Heisenberg spin pairs, namely from the antiparallel oriented Heisenberg spin pair (one spin in $S^z = -1$ state, another one in spin $S^z = 1$ state to be further denoted as the '1–1' spin pair) towards the spin pair with both Heisenberg spins in the spin $S^z = 0$ state (the '00' spin pair). However, in the large Δ limit both types of Heisenberg spin pair ('1–1' as well as '00') are equally well populated and with a high probability also randomly distributed among Ising spins. This suggestion is strongly supported by results for the correlation q_{ih}^{zz} and staggered magnetization m_B^s which asymptotically tend to zero as $\Delta \to \infty$ (figure 8(a)). Finally, one should also notice that all these effects could originate from the onset of the AF short-range ordering in the xy plane

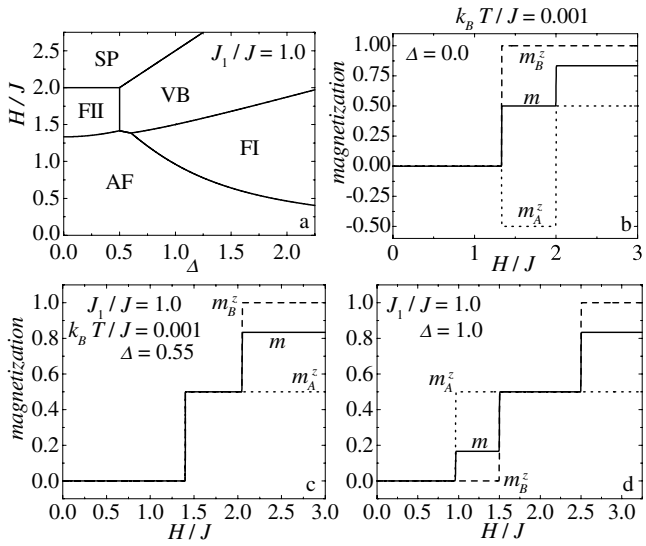

Figure 7. Ground-state phase diagram together with some typical examples of low-temperature magnetization curves when the ratio $J_1/J = 1.0$: (a) ground-state phase diagram in the Δ–H/J plane; (b)–(d) some typical examples of the low-temperature ($k_BT/J = 0.001$) magnetization curves for various anisotropies Δ.

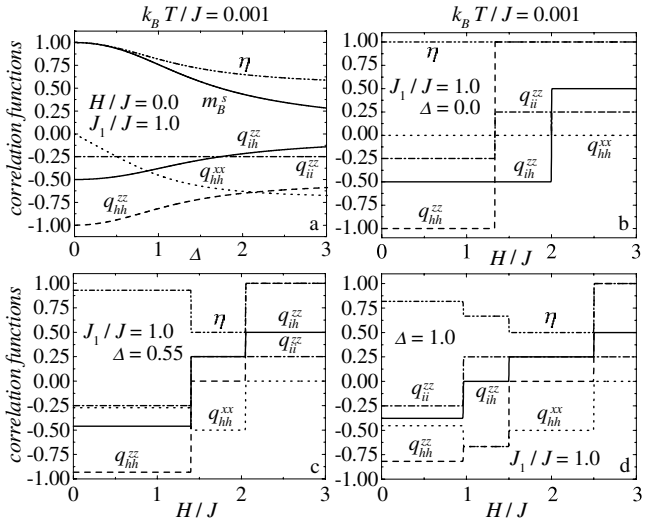

Figure 8. Low-temperature ($k_BT/J = 0.001$) behaviour of several correlation functions q_{hh}^{zz} (dashed), q_{hh}^{xx} (dotted), q_{ih}^{zz} (solid), q_{ii}^{zz} (dashed–dotted), quadrupolar momentum η (dashed–dotted–dotted) and staggered sublattice magnetization m_B^s (solid curve): (a) zero-field variations of relevant quantities with anisotropy Δ; (b)–(d) field-dependences of correlations for selected values of Δ.

(nonzero q_{hh}^{xx}) that is the stronger (up to the value $1/\sqrt{2}$) the greater the exchange anisotropy strength Δ.

Now, let us turn our attention to both the FI and FII ferrimagnetic phases. As in the spin $S = 1/2$ case, the nonzero total magnetization of the FI phase arises due to the fully

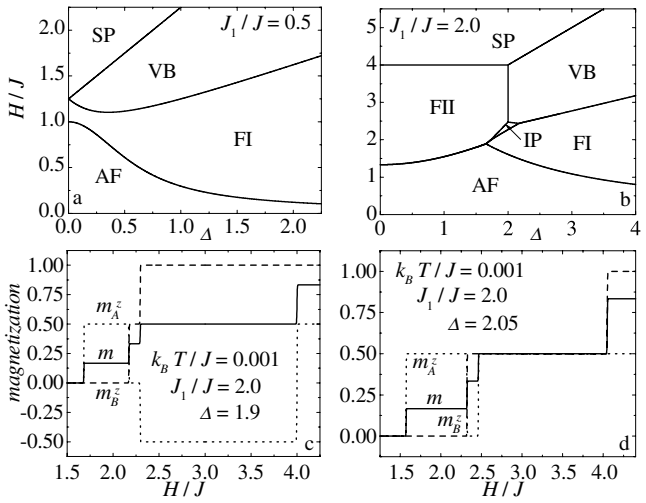

Figure 9. Ground-state phase diagrams together with some typical examples of low-temperature magnetization curves: (a), (b) ground-state phase diagram in the Δ–H/J plane for $J_1/J = 0.5$ and 2.0; (c), (d) some typical examples of the low-temperature ($k_B T/J = 0.001$) magnetization curves when $J_1/J = 2.0$ and $\Delta = 1.9$ and 2.05 respectively.

polarized Ising spins only ($m_A^z = 1/2$ and $q_{ii}^{zz} = 1/4$), while the Heisenberg sublattice does not contribute to the total magnetization at all ($m_B^z = 0$ and $q_{ih}^{zz} = 0$). Since the FI phase can arise by increasing the external field from the AF phase only (see figures 7(a), 9(a), (b)), it is of interest to compare the relevant spin ordering in both phases. Actually, one still finds $\eta = |q_{hh}^{zz}|$ to be valid, but the nearest-neighbour correlation $q_{hh}^{zz}(q_{hh}^{xx})$ is weaker (stronger) in the FI phase with respect to that in the AF phase (figure 8(d)). These results are taken to mean that the number of nearest-neighbour '00' spin pairs increases (of course, only up to one-half of the total number of pairs) as one passes through the AF–FI phase boundary. Moreover, the appearance of a massive short-range order in the xy plane strongly implies the relevance of local quantum fluctuations also in the FI phase. On the other hand, in the second ferrimagnetic phase FII we have found the following results

$$(q_{hh}^{xx}, q_{hh}^{zz}, q_{ih}^{zz}, q_{ii}^{zz}, \eta, m_A^z, m_B^z, m) = (0, 1, -1/2, 1/4, 1, -1/2, 1, 1/2),$$

indicating the 'classical' character of this phase that is usually observed in pure Ising spin systems as well. As the relevant spin ordering is thoroughly analogous to that in the FII phase of the spin $S = 1/2$ chain, for brevity we will not repeat its description here.

The most interesting spin order, however, can be found in the valence-bond (VB) phase and the intermediate phase (IP). Actually, for instance in the VB phase, one finds

$$(q_{hh}^{xx}, q_{hh}^{zz}, q_{ih}^{zz}, q_{ii}^{zz}, \eta, m_A^z, m_B^z, m) = (-1/2, 0, 1/4, 1/4, 1/2, 1/2, 1/2, 1/2).$$

As one can see, in contrast to the fully polarized Ising sublattice ($m_A^z = 1/2$ and $q_{ii}^{zz} = 1/4$), each couple of the nearest-neighbour Heisenberg spins consists of one polarized spin ($S^z = 1$) and one spin in the $S^z = 0$ state, i.e. the spin-'01' pair. It is interesting to note that the symmetrization of both Heisenberg spin states can be achieved using the valence-bond-solid (VBS) picture [12]. Accordingly, each spin-1 atom splits into one polarized spin-1/2 variable with the fixed projection into the external field direction and one spin-1/2 variable with the unfixed projection creating a valence bond. Thus, it is reasonable to assume that both Heisenberg spins interchange their spin states (tunnelling between the $S^z = 0$ and 1 spin

states) and therefore, they effectively act on the surrounding Ising spins as the spin-1/2 atoms (see also the result for correlation q_{ih}^{zz}). However, the AF short-range order in the xy plane (nonzero q_{hh}^{xx}), as well as the fact that the VB phase cannot be detected in the pure Ising system (i.e. for $\Delta = 0$), imply again the obvious influence of the local quantum fluctuations.

Perhaps the most striking spin alignment has been discovered in the IP phase. Among other things, the perfect AF alignment between the Ising spins ($m_A^s = 1/2$ and $q_{ii}^{zz} = -1/4$) has been confirmed in the IP phase, hence the total magnetization of the system ($m = 1/3$) is entirely determined by the contribution of Heisenberg spins. Anyway, the results for the Heisenberg sublattice magnetization $m_B^z = 1/2$, correlation function $q_{hh}^{zz} = 0$ and quadrupolar momentum $\eta = 1/2$, clearly indicate that each couple of nearest-neighbour Heisenberg atoms comprises the spin-'01' pair. However, since both Heisenberg spins are placed in the IP phase between two non-equivalent Ising spins (one 'up', other 'down'), the spin state interchange between both Heisenberg atoms would lead to $q_{ih}^{zz} = 0$ which is in contradiction with our numerical result $q_{ih}^{zz} \neq 0$. On the other hand, if the Heisenberg atom in the spin $S^z = 1$ state were to be strictly antiferromagnetically coupled to its nearest-neighbour Ising spin (spin 'down'), then we would have $q_{ih}^{zz} = -1/4$. Nevertheless, our result for the correlation $|q_{ih}^{zz}| \ll 1/4$ indicates only partial AF order between Ising and Heisenberg spins. This observation would suggest that the spin-'01' Heisenberg pairs should be, to a certain degree, randomly distributed among Ising spins. Finally, as one would expect, in the high-field limit the system undergoes a phase transition towards the fully SP phase. As before, in the SP phase all Ising and Heisenberg spins are completely aligned towards the direction of the external field, thus in the SP phase one attains

$$(q_{hh}^{xx}, q_{hh}^{zz}, q_{ih}^{zz}, q_{ii}^{zz}, \eta, m_A^z, m_B^z, m) = (0, 1, 1/2, 1/4, 1, 1/2, 1, 5/6).$$

Now, let us proceed to examine the magnetization process of the system under investigation. For this purpose, we have shown in figures 7(a) and 9(a), (b) the ground-state phase diagrams in the Δ–H/J plane together with some typical examples of the magnetization curves (figures 7(b)–(d) and 9(c), (d)) for three selected values of interaction parameters J_1/J. In order to provide an independent check of the magnetization scenario from figures 7(b)–(d), the corresponding field dependences of the correlation functions and quadrupolar momentum are displayed in figures 8(b)–(d). Obviously, all the above results are absolutely in accordance with the aforementioned ground-state spin ordering. Moreover, through the comparison of figures 7(a) and 9(a), (b) one can realize that the nature of magnetization process depends basically on the ratio between the Ising and Heisenberg interaction parameters. In fact, the stronger the Ising interaction J_1 with respect to the Heisenberg one $J(\Delta)$, the broader the parameter region corresponding to the 'classical' FII phase. Otherwise, the increasing influence of the Heisenberg interaction $J(\Delta)$ causes the broadening of regions corresponding to the FI and VB phase respectively, until the FII phase completely vanishes below $J_1/J < 2/3$ (see e.g. figure 9(a) where the FII phase is already missing). Consequently, in the FI and VB phases one can expect that the effect of local quantum fluctuations plays an important role.

Although, the system exhibits a stepwise magnetization curve with an abrupt change of the magnetization in the whole range of parameters (see figures 7(b)–(d) and 9(c), (d)), there is a fundamental difference between the magnetization process in the 'classical' Ising-like regime and that in the quantum regime. As a matter of fact, in the former case one observes the double-plateau magnetization curve with the FII plateau state only, i.e. with the FII phase as an intermediate state between the AF and SP phase (see figure 7(b)). Contrary to this, in the latter case one can detect the double- (figure 7(c)), triple- (figure 7(d)) or quadruple-plateau (figures 9(c), (d)) magnetization curves. The double-plateau magnetization curves are rather rarely observable, since they arise due to the direct metamagnetic transition from the AF phase

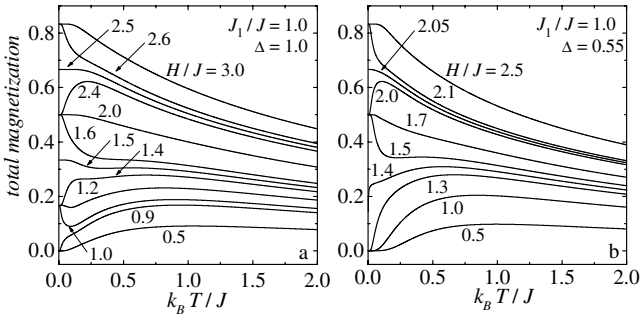

Figure 10. Thermal variations of the total magnetization for $J_1/J = 1.0$ and two selected values of Δ.

to the VB phase in a relatively narrow region of Δ only (see figure 7(a)). However, when the mechanism of the magnetization process is driven by the Heisenberg interaction, i.e. under the requirement of sufficiently small J_1/J and sufficiently large Δ, the triple-plateau magnetization curves with the transitions between AF–FI–VB–SP phases are always preferred (figure 7(d)). Finally, one should also remark that if the condition $\Delta \approx H/J \approx J_1/J > 1$ is satisfied, there also appear the extraordinary quadruple-plateau magnetization curves (see figure 9(b)) with the IP phase in a very narrow region of the external field. Indeed, we even found two different possibilities for the quadruple–cascade transitions, namely the AF–FI–IP–FII–SP cascade transitions (figure 9(c)) and the AF–FI–IP–VB–SP ones (figure 9(d)).

To conclude the analysis of the spin $S = 1$ chain, we will also briefly mention the finite-temperature behaviour of the system under consideration. For this purpose, the thermal variations of the total magnetization are plotted in figure 10 for $J_1/J = 1.0$ and two selected values of the anisotropy Δ. In agreement with the aforementioned arguments, one observes here three and two field-induced transitions for the anisotropy strengths $\Delta = 1.0$ and 0.55 respectively. Evidently, as the magnitude of the external field varies, the various thermal dependences result from competition between the Ising interaction, Heisenberg interaction and magnetic field. However, the most interesting dependences arise again for the external fields from the vicinity of the phase boundaries. In such a case, the relevant thermal excitations result in a very rapid change of magnetization due to the competing influence of the phases separated by the relevant transition line. Moreover, it turns out that the narrower the interval of external fields corresponding to the relevant phase, the more robust the change in the magnetization that can be observed.

4. Conclusion

In the present paper we have obtained the exact solution of the mixed spin-1/2 and spin-S ($S = 1/2, 1$) Ising–Heisenberg chain in an external magnetic field. The most important result stemming from this study is the confirmation of a multistep magnetization process by an exact calculation. Moreover, it has been proved that the character of the magnetization process depends essentially on the ratio between the Ising and Heisenberg interactions, whereas the *XXZ* anisotropy term Δ also allows it to be controlled in a decisive manner. Since the presence of the nondiagonal interaction term $J\Delta$ is responsible for the onset of the local quantum fluctuations, as we have also shown, it basically modifies an otherwise trivial Ising-like behaviour. For example, in the case of the spin $S = 1$ chain one finds instead of the double-plateau magnetization curve arising in the pure Ising spin system ($\Delta = 0$), double-,

triple- or even quadruple-plateau magnetization curves in the Ising–Heisenberg chain with $\Delta \neq 0$. Altogether, the presented results indicate that extraordinarily rich ground-state phase diagrams result from the competition between the easy-axis interactions J_1, J and the easy-plane interaction $J\Delta$.

One should also emphasize that our research on Ising–Heisenberg chains has been stimulated by the recent experimental works dealing with many quasi-1D mixed-spin chains [13]. Although we are not aware of any quasi-1D system in which two kinds of magnetic ions regularly alternate with $p = 3$ periodic fashion (AABAAB...), the recent progress in molecular engineering [14] supports our hope that the synthesis of such a polymeric chain should be possible in the near future. Structural derivatives of a novel polymeric chain recently reported by Mukherjeee *et al* [15], seem to be the most promising candidates from this point of view. In fact, the crystal structure of the above-mentioned polymeric chain consists of the spin-1/2 Cu^{II} dimers linked through Ni^{II} monomers. Unfortunately, as a consequence of the square-planar coordination of Ni^{II} ions in $[Ni^{II}(CN)_4]^{2-}$ bridging groups, the Ni^{II} metal ions are diamagnetic and thus, they do not contribute to the magnetism.

Finally, it should be stressed that the applied mapping transformation technique does not require any restriction to the dimensionality of the spin system, and hence it can be straightforwardly generalized to the mixed Ising–Heisenberg lattices in two and three dimensions too [10].

Acknowledgments

The authors would like to thank the referees for useful comments. This work was supported by the VEGA grant no 1/9034/02 and APVT grant no 20-009902.

Appendix. Explicit expressions for the functions V_1–V_7

(a) Spin-1/2 chain.

$$V_1 = 2\exp(-\beta J/4)\cosh(\beta J_1/2 + \beta H_B) + 2\exp(\beta J/4)\cosh(\beta J\Delta/2)$$
$$V_2 = 2\exp(-\beta J/4)\cosh(\beta J_1/2 - \beta H_B) + 2\exp(\beta J/4)\cosh(\beta J\Delta/2)$$
$$V_3 = 2\exp(-\beta J/4)\cosh(\beta H_B) + 2\exp(\beta J/4)\cosh\Big(\beta\sqrt{J_1^2 + (J\Delta)^2}/2\Big)$$
$$V_4 = \exp(-\beta J/4)\sinh(\beta J_1/2 + \beta H_B)/2$$
$$V_5 = \exp(-\beta J/4)\sinh(\beta J_1/2 - \beta H_B)/2$$
$$V_6 = \exp(-\beta J/4)\sinh(\beta H_B)/2,$$
$$V_7 = \frac{2J_1\exp(\beta J/4)}{\sqrt{J_1^2 + (J\Delta)^2}}\sinh\Big(\beta\sqrt{J_1^2 + (J\Delta)^2}/2\Big).$$

(b) Spin-1 chain.

$$V_1 = 2\exp(-\beta J)\cosh(\beta J_1 + 2\beta H_B) + \exp(2\beta J/3)W_1 + 4\cosh(\beta J_1/2 + \beta H_B)\cosh(\beta J\Delta)$$
$$V_2 = 2\exp(-\beta J)\cosh(\beta J_1 - 2\beta H_B) + \exp(2\beta J/3)W_1 + 4\cosh(\beta J_1/2 - \beta H_B)\cosh(\beta J\Delta)$$
$$V_3 = 2\exp(-\beta J)\cosh(2\beta H_B) + \exp(2\beta J/3)W_2 + 4\cosh(\beta H_B)\cosh\Big(\beta\sqrt{J_1^2 + (2J\Delta)^2}/2\Big)$$

$$V_4 = \exp(-\beta J)\sinh(\beta J_1 + 2\beta H_B) + \sinh(\beta J_1/2 + \beta H_B)\cosh(\beta J\Delta)$$
$$V_5 = \exp(-\beta J)\sinh(\beta J_1 - 2\beta H_B) + \sinh(\beta J_1/2 - \beta H_B)\cosh(\beta J\Delta)$$
$$V_6 = \exp(-\beta J)\sinh(2\beta H_B) + \sinh(\beta H_B)\cosh\Big(\beta\sqrt{J_1^2 + (2J\Delta)^2}/2\Big)$$

where the expressions W_1 and W_2 are given by:

$$W_1 = \sum_{n=0}^{2} \exp\{-2\beta P_1 \cos[(\phi_1 + 2\pi n)/3]\},$$
$$W_2 = \sum_{n=0}^{2} \exp\{-2\beta P_2 \cos[(\phi_2 + 2\pi n)/3]\},$$
$$P_1^2 = (J/3)^2 + 2(J\Delta)^2/3, \qquad P_2^2 = (J/3)^2 + 2(J\Delta)^2/3 + J_1^2/3,$$
$$Q_1 = (J/3)^3 + J(J\Delta)^2/3, \qquad Q_2 = (J/3)^3 + J(J\Delta)^2/3 - J_1^3,$$
$$\phi_1 = \arctan\Big(\sqrt{P_1^6 - Q_1^2}/Q_1\Big), \qquad \phi_2 = \arctan\Big(\sqrt{P_2^6 - Q_2^2}/Q_2\Big).$$

References

[1] Haldane F D M 1983 *Phys. Lett.* A **93** 464
Haldane F D M 1983 *Phys. Rev. Lett.* **50** 1153
[2] Lieb E H, Schultz T D and Mattis D C 1961 *Ann. Phys., NY* **16** 407
Lieb E H and Mattis D C 1962 *J. Math. Phys.* **3** 749
[3] Oshikawa M, Yamanaka M and Affleck I 1997 *Phys. Rev. Lett.* **78** 1984
Affleck I 1998 *Phys. Rev.* B **37** 5186
[4] Zvyagin A A 1990 *Sov. Phys.–Solid State* **32** 181
Hida K 1994 *J. Phys. Soc. Japan* **63** 2359
Okamoto K 1995 *Solid State Commun.* **98** 245
Tonegawa T, Nakao T and Kaburagi H 1996 *J. Phys. Soc. Japan* **65** 3317
Pati S K, Ramasecha S and Sen D 1997 *Phys. Rev.* B **55** 8894
Sakai T and Takahashi M 1998 *Phys. Rev.* B **57** R3201
Totsuka K 1997 *Phys. Lett.* A **228** 103
Totsuka K 1998 *Phys. Rev.* B **57** 3454
Sakai T and Yamamoto S 1999 *Phys. Rev.* B **60** 4053
Yamamoto S and Sakai T 2000 *Phys. Rev.* B **62** 3795
Okamoto K and Kitazawa A 1999 *J. Phys. A: Math. Gen.* **32** 4601
Kitazawa A and Okamoto K 1999 *J. Phys.: Condens. Matter* **11** 9765
Koga A, Okunishi K and Kawakami N 2000 *Phys. Rev.* B **62** 5558
Sakai T and Okamoto K 2002 *Phys. Rev.* B **65** 214403
Schulenburg J and Richter J 2002 *Phys. Rev.* B **65** 054420
Chen X Y, Jiang Q and Wu Y Z 2002 *Solid State Commun.* **121** 641
[5] Bethe H A 1931 *Z. Phys.* **71** 205
Hulthén L 1938 *Ark. Mat. Astron. Phys.* A **26** 1
Orbach R 1958 *Phys. Rev.* **112** 309
des Cloizeaux J and Gaudin M 1966 *J. Math. Phys.* **7** 1384
Yang C N and Yang C P 1966 *Phys. Rev.* **150** 321
Yang C N and Yang C P 1966 *Phys. Rev.* **150** 327
Yang C N and Yang C P 1966 *Phys. Rev.* **151** 258
Majumdar C K and Ghosh D K 1969 *J. Math. Phys.* **10** 1388
Majumdar C K and Ghosh D K 1969 *J. Math. Phys.* **10** 1399
Majumdar C K 1970 *J. Phys. C: Solid State Phys.* **3** 911
Kirillov A N and Reshetikhin N Yu 1987 *J. Phys. A: Math. Gen.* **20** 1565
Kirillov A N and Reshetikhin N Yu 1987 *J. Phys. A: Math. Gen.* **20** 1587
Parkinson J B 1989 *J. Phys.: Condens. Matter* **1** 6709
Long M W and Fehrenbacher R 1990 *J. Phys.: Condens. Matter* **2** 2787

Long M W and Siak S 1990 *J. Phys.: Condens. Matter* **2** 10321
de Vega H J and Woynarovich F 1990 *J. Phys. A: Math. Gen.* **23** 1613
Kubo K 1993 *Phys. Rev.* B **48** 10552
[6] de Vega H J and Woynarovich F 1992 *J. Phys. A: Math. Gen.* **25** 4499
Martins M J 1993 *J. Phys. A: Math. Gen.* **26** 7301
Dörfel B D and Meissner St 1996 *J. Phys. A: Math. Gen.* **29** 1949
Dörfel B D and Meissner St 1996 *J. Phys. A: Math. Gen.* **29** 6471
Dörfel B D and Meissner St 1997 *J. Phys. A: Math. Gen.* **30** 1931
Dörfel B D and Meissner St 1998 *J. Phys. A: Math. Gen.* **31** 61
Dörfel B D and Meissner St 1999 *J. Phys. A: Math. Gen.* **32** 41
Zvyagin A A 1990 *J. Phys. A: Math. Gen.* **34** R21
[7] Yao H, Li J and Gong Ch D 2002 *Solid State Commun.* **121** 687
[8] Syozi I 1972 *Phase Transition and Critical Phenomena* vol 1, ed C Domb and M S Green (New York: Academic)
[9] Lavis D A and Bell G M 1999 *Statistical Mechanics of Lattice Systems* vol 1 (Berlin: Springer)
[10] Strečka J and Jaščur M 2002 *Phys. Rev.* B **66** 174415
Jaščur M and Strečka J 2002 *Acta Electrotechnica et Informatica* **2** 71
Strečka J and Jaščur M 2002 *Phys. Status Solidi* b **233** R12
[11] Strečka J and Jaščur M 2002 *Czech. J. Phys.* **52** A37
[12] Affleck I, Kennedy T, Lieb E H and Tasaki H 1987 *Phys. Rev. Lett.* **59** 799
[13] Gleizes A and Verdauger M 1981 *J. Am. Chem. Soc.* **103** 7373
Verdauger M, Julve M, Michalowicz A and Kahn O 1983 *Inorg. Chem.* **22** 2624
Drillon M, Gianduzzo J C and Gorges R 1983 *Phys. Lett.* A **96** 413
Gleizes A and Verdauger M 1984 *J. Am. Chem. Soc.* **106** 3727
Verdauger M, Gleizes A, Renard J P and Seiden J 1984 *Phys. Rev.* B **29** 5144
Gorges R, Drillon M and Currely J 1985 *J. Appl. Phys.* **58** 914
Kahn O 1987 *Struct. Bonding (Berlin)* **68** 91
Pei Y, Verdauger M, Kahn O, Sletten J and Renard J P 1987 *Inorg. Chem.* **26** 138
Kahn O, Pei Y, Verdauger M, Renard J P and Sletten J 1988 *J. Am. Chem. Soc.* **110** 782
Pei Y, Kahn O, Sletten J, Renard J P, Georges R, Gianduzzo J C, Curely J and Xu Q 1988 *Inorg. Chem.* **27** 47
Caneschi A, Gatteschi D, Renard J P, Rey P and Sessoli R 1989 *Inorg. Chem.* **28** 1976
Van Koningsbruggen P J, Kahn O, Nakatani K, Pei Y, Renard J P, Drillon M and Leggol P 1990 *Inorg. Chem.* **29** 3325
Kahn O, Pei Y and Journaux Y 1995 *Inorganic Materials* ed D W Bruce and D O'Hare (New York: Wiley)
Hagiwara M, Minami K, Narumi Y, Tatani K and Kindo K 1998 *J. Phys. Soc. Japan* **67** 2209
[14] Willet R D, Wang Z, Molnar S, Brewer K, Landee C P, Turnbull M M and Zhang W 1993 *Mol. Cryst. Liq. Cryst.* **233** 277
Kahn O 1993 *Molecular Magnetism* (New York: Wiley–VCH)
Verdauger M 2001 *Polyhedron* **20** 1115
Černák J, Orendáč M, Potočňák I, Chomič J, Orendáčová A, Skoršepa J and Feher A 2002 *Coord. Chem. Rev.* **224** 51
[15] Mukherjeee P S, Maji T K, Mallah T, Zangrando E, Randaccio L and Chaudhuri N R 2001 *Inorg. Chim. Acta* **315** 249